Orientational changes of supported chiral 2,2 '-dihydroxy-1,1 ' binaphthyl molecules

ARTICLE *in* PHYSICAL CHEMISTRY CHEMICAL PHYSICS · MARCH 2014

Impact Factor: 4.49 · DOI: 10.1039/c4cp00106k · Source: PubMed

PCCP

PAPER

View Article Online
View Journal | View Issue

Cite this: *Phys. Chem. Chem. Phys.*, 2014, **16**, 7299

Orientational changes of supported chiral 2,2′-dihydroxy-1,1′binaphthyl molecules

Philipp Heister,[a] Tobias Lünskens,[a] Martin Thämer,[b] Aras Kartouzian,[a] Sabine Gerlach,[a] Thierry Verbiest[c] and Ueli Heiz*[a]

Received 9th January 2014,
Accepted 12th February 2014

DOI: 10.1039/c4cp00106k

www.rsc.org/pccp

Well defined thin molecular films of 2,2′-dihydroxy-1,1′binaphthyl (binol) molecules at coverages between 5×10^{15} molecules per cm^2 and 10^{17} molecules per cm^2 on thin glass (BK7) substrates were investigated under ultra-high-vacuum (UHV) conditions. Second-Harmonic-Generation Optical-Rotatory-Dispersion measurements (SHG-ORD) were performed using a dedicated spectroscopic setup which allows for the determination of the rotation angle of the SH-signal of two enantiomers. Rotation angles of up to 38 degrees were measured. The chirality of the two enantiomers has been studied at 674 nm (337 nm resonance wavelength) in the transmission mode. Coverage dependent orientation evolution of binol molecular films was revealed by precise monitoring of the surface coverage while performing SHG-ORD experiments. We show that the molecules reach their final orientation at a surface coverage of 5×10^{16} molecules per cm^2. From the obtained experimental data the ratio of chiral and achiral susceptibility components could be calculated and was observed to change with coverage.

Introduction

Systems are chiral if their mirror image cannot be brought to coincide with themselves.[1] Therefore, chiral molecules exist in two forms (enantiomers), which are mirror images of each other. Due to its great scientific importance in biochemistry, pharmacology and catalysis, chirality has been a widely studied phenomenon.[2] In 1812 Jean Baptiste Biot was the first to observe the rotation of the polarization of linearly polarized light by chiral molecules.[3] This effect is called linear optical rotation. In linear optics, where the applied electric field is weak compared to internuclear atomic fields, measurements of circular dichroism and linear optical rotation are techniques that are often used to probe chiral molecules in solutions or in the gas phase.[4,5] Those effects do not depend on the intensity of light and their origin lies in the different complex refractive indices for left- and right circularly polarized light. This, however, is only the case if one goes beyond the electric dipole approximation and magnetic contributions are included. Nonlinear effects occur, if the applied electric field intensities are comparable to internuclear atomic fields. Nowadays this is often the case when pulsed lasers are used. In this case, and in contrast to linear optics, nonlinear optical activity can occur within the electric dipole approximation without considering magnetic transitions.[6] For increasing field intensities even higher order, *e.g.* cubic or quadratic contributions were observed.[7]

The enantiomeric atropisomers of 2,2′-dihydroxyl-1,1′binaphthyl (binol) are widely used ligands for both stoichiometric and catalytic asymmetric reactions.[8] Binol has also often been used as a chiral probe molecule on surfaces.[9–12] Furthermore it was indeed shown that nonlinear effects in binol are dominated by electric dipole transitions.[6] This is typical for those molecules, which are composed of two identical components, spatially arranged in a nonmirror symmetric configuration.[13] In this publication we focus on the second order nonlinear process within the electric dipole approximation. This simplifies the theoretical description to a great extent by neglecting magnetic contributions. However, it should be pointed out that this assumption is not valid for all chiral molecules.[14–16]

Surface Second Harmonic Generation (s-SHG) is a very powerful and sensitive tool to investigate thin films of adsorbates on surfaces and has been used for many years since Shen and co-workers presented their first experiments.[17] The high sensitivity of this nonlinear technique originates from its surface sensitive character when used with centro-symmetric or amorphous substrates.[18–20]

Second Harmonic Generation Optical Rotatory Dispersion (SHG-ORD) is a nonlinear analogue of linear optical rotation. Linearly p-polarized fundamental light is used as an excitation source while the polarization of the detected SHG light is measured. The phase difference between p-polarized light and polarization of the detected SHG-light is called rotation angle ϕ. The major advantage of this background-free technique is the

[a] *Lehrstuhl für physikalische Chemie & Catalysis Research Center, Chemistry Department, Technische Universität München, Lichtenbergstraße 4, 85748 Garching bei München, Germany. E-mail: ulrich.heiz@mytum.de*
[b] *Department of Chemistry, University of Chicago, Chicago, Illinois 60637, USA*
[c] *Chemistry Department, University of Leuven, Celestijnenlaan 200 D, B-3001 Leuven, Belgium*

combination of the high sensitivity of s-SHG and the chiral sensitive effect of optical rotation. SHG-ORD is easy to implement and not constrained to resonant wavelengths.[2] Remarkably, the nonlinear chiral effect can be up to 6 orders of magnitude larger than its linear counterpart.[7] Pioneering work on second harmonic generation circular dichroism (SHG-CD) and SHG-ORD on ultrathin films at fused silica and liquid interfaces was carried out independently by the Hicks group and the Persoons group in the 1990s.[9,10,21–24] In recent years s-SHG has been used to investigate surface chirality and has been applied to biological, chemical and artificial systems.[2,7,25,26]

To the best of our knowledge no work has been reported on well-characterized thin molecular films of chiral molecules under UHV conditions by nonlinear techniques. In particular, coverage dependent nonlinear chiral response has not been investigated or observed. In the following we show that monitoring coverage, however, is crucial to obtain definite SHG-ORD results for such film thicknesses.

Chiral molecular films on solid surfaces are of potential interest for several applications. When depositing small metal clusters onto such surfaces it is assumed that the chirality is transmitted to the clusters as is the case for ligand protected clusters.[27–29] This combination of deposited metal clusters or nanoparticles with chiral molecules might however be crucial for triggering, for example, heterogeneous enantioselective catalysis under stable and well-defined conditions. Also, for the design of nonlinear chiroptical devices a deep insight into the link between the molecular origin of chiral effects, given by the molecular hyperpolarizability $\alpha^{(2)}$, and the macroscopic behaviour of these materials is of great scientific interest.

In this work we employ a setup, which allows for the preparation of well-characterized molecular thin films and the nonlinear spectroscopic characterisation of chiral materials on transparent insulating substrates under UHV conditions. We show that coverage dependent measurements are crucial in order to understand their chiroptical response. We furthermore show that for binol in-plane isotropy is valid for the investigated sample and the molecules change their orientation with coverage. We finally calculate the ratio of chiral to achiral tensor components for different coverages.

Theoretical aspects

Within the electric dipole approximation, the second harmonic response of an insulator is given by the nonlinear polarization

$$P_i^{(2)}(2\omega) = \sum_{j,k} \varepsilon_0 \chi_{ijk}^{(2)} E_j(\omega) E_k(\omega) \qquad (1)$$

Here, ε_0 is the permittivity of vacuum, ω is the frequency of the applied electric field, and $\chi_{ijk}^{(2)}$ are the components of the second order susceptibility tensor. $\chi^{(2)}$ is a third rank tensor and contains $3 \times 3 \times 3 = 27$ elements. From this formula, it follows that SHG can only be generated at regions without inversion symmetry, such as nonlinear crystals or surfaces and interfaces.[17] SHG is therefore a surface sensitive technique and is often used to probe adsorbed molecules on surfaces. In the following we use the experimental coordinate system shown in Fig. 1. Here, p-polarized light is defined as the polarization in the *xz*-plane, and consequently s-polarized light is the polarization normal to the *xz*-plane. The interface normal is parallel to the *z*-axis. In this coordinate system the number of tensor components can significantly be reduced by symmetry considerations.

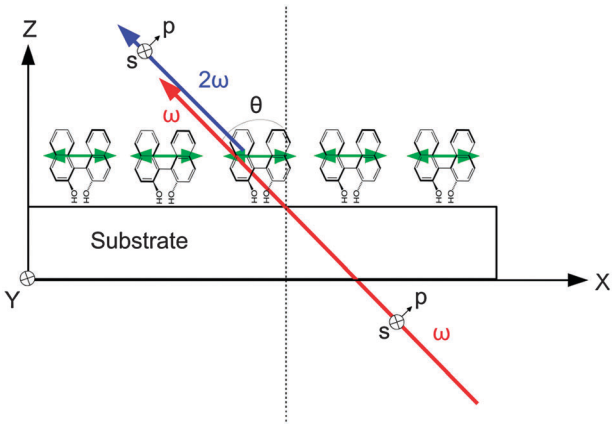

Fig. 1 Coordinate system. Here, only the transmission mode (A) is shown, and the molecules are assumed to be oriented with their hydroxyl groups towards the surface.

For a chiral rotationally isotropic surface (C_∞ symmetry) only 11 components of $\chi_{ijk}^{(2)}$ are nonzero. However, as not all of these components are independent, the number can be reduced to only 4 independent nonzero components,[2] given by $\chi_1 = \chi_{zzz}^{(2)}$, $\chi_2 = \chi_{zxx}^{(2)} = \chi_{zyy}^{(2)}$, $\chi_3 = \chi_{xxz}^{(2)} = \chi_{yyz}^{(2)} = \chi_{yzy}^{(2)} = \chi_{xzx}^{(2)}$, $\chi_4 = \chi_{xyz}^{(2)} = -\chi_{yxz}^{(2)} = -\chi_{yzx}^{(2)} = \chi_{xzy}^{(2)}$. For an achiral (racemic) surface, reflection is an additional symmetry operation. This causes the elimination of χ_4, and only 3 tensor components remain. χ_1, χ_2 and χ_3 are nonzero for all isotropic surfaces and are therefore referred to as achiral tensor components. χ_4 is only nonzero for chiral surfaces, and is therefore referred to as the chiral tensor component. The appearance of nonlinear chiroptical effects (such as SHG-ORD) is consequently connected to this tensor component. As shown in the following the second harmonic field $E(2\omega)$ can be written in terms of s- and p-polarized components of the fundamental field $E(\omega)$:[14]

$$E_i(2\omega) = f_i E_p^{\,2}(\omega) + g_i E_s^{\,2}(\omega) + h_i E_p(\omega) E_s(\omega) \qquad (2)$$

where i is the s- or p-component of the induced electric field $E(2\omega)$. f, g and h can be considered as susceptibility components in the p–s basis, which also include Fresnel factors. For a chiral isotropic surface within the electric dipole approximation and taking linear refractive indices to be unity, coefficients f, g and h can be related to the susceptibility components in the *xyz* coordinate system *via*:[14]

$$f_s = 2\chi_4 \sin\theta \cos\theta$$

$$g_s = 0$$

$$h_s = 2\chi_3 \sin\theta$$

$$f_p = (\chi_1 \sin^2\theta + \chi_2 \cos^2\theta + 2\chi_3 \cos^2\theta)\sin\theta$$

$$g_p = \chi_2 \sin\theta$$
$$h_s = -2\chi_4 \sin\theta\cos\theta \quad (3)$$

For p-polarized fundamental light the rotation angle ϕ can be expressed as the ratio of f_s and f_p and is given by:

$$\phi = \tan^{-1}\left(\frac{f_s}{f_p}\right) = \tan^{-1}\left(\frac{2\chi_4\cos\theta}{\chi_1\sin^2\theta + (\chi_2 + 2\chi_3)\cos^2\theta}\right) \quad (4)$$

f_s reverses the sign between two enantiomers because it includes the chiral component χ_4, whereas f_p does not change the sign between enantiomers because it includes only achiral tensor components (χ_1, χ_2, and χ_3). As a consequence, the rotation angle ϕ changes sign when interchanging the two different enantiomers of a chiral molecule. The magnitude of the SHG-ORD effect obviously depends on the ratio between the components f_s and f_p. It can be seen that the rotation angle is limited to $\phi = \pm 90^\circ$ and that for $f_s = 0$ no rotation occurs. The rotation angle ϕ will be large when f_s (given by χ_4) is large compared to f_p. It can also be seen that the rotation angle ϕ will decrease with increasing incident angle. The SHG signal of the film on the surface, however, depends on the incident angle[19] $I(\omega) \sim \sec^2\theta$. For a good signal to noise ratio of the rotation angle one must therefore balance the SHG signal intensity *versus* the magnitude of the rotation angle ϕ. $\chi^{(2)}$, however, is a macroscopic quantity and depends on the spatial arrangement of the molecular hyperpolarizabilities $\alpha^{(2)}$. For non-interacting molecules (local field corrections are neglected) $\chi^{(2)}$can be expressed as:[30]

$$\chi^{(2)}_{ijk} = N_s \sum_{abc} T_{ia} T_{jb} T_{kc} \alpha^{(2)}_{abc} \quad (5)$$

where N_s is the number density of surface molecules and T_{ia} represents the projection of the lab frame coordinates i, j, and k onto the molecular coordinates a, b, and c. The brackets $\langle\rangle$ represent the average over all orientations of the surface molecules. In order to determine $T_{i,a}$, $T_{j,b}$, and $T_{k,c}$ one needs to know both the nonlinear susceptibility tensor $\chi^{(2)}$ and the nonlinear hyperpolarizability $\alpha^{(2)}$. While $\chi^{(2)}$ is often easy to measure by s-SHG, $\alpha^{(2)}$ is usually difficult to obtain. Therefore, it is very challenging to determine the average orientation of the molecules on the surface.[6,9,31] According to eqn (5) the macroscopic nonlinear susceptibility $\chi^{(2)}$ is related to the molecular hyperpolarizability $\alpha^{(2)}$ and the average orientation of the molecules in the system. Therefore, the macroscopic susceptibility tensor $\chi^{(2)}$ changes with any changes in the orientation distributions of the molecules.

In the presented work, two different geometric alignments and accordingly transmission modes are used (A: substrate/molecule and B: molecule/substrate). In order to understand the behaviour of the SHG-ORD effect and the sign of the rotation angle, a deeper look into the properties of the nonlinear susceptibility $\chi^{(2)}$ for different orientations in respect of the propagating electric field (two transmission modes) is useful. It can be shown that inverting the molecules by a C_2 rotation around the x-axis (this is similar to switching from transmission mode A to transmission mode B), the achiral tensor elements χ_1, χ_2, and χ_3 change signs, while the chiral tensor element χ_4 does not.[10] Interchanging of enantiomers, however, only affects the chiral tensor element and changes its sign ($\chi_4 \rightarrow -\chi_4$). Hence it is important to note that in an SHG-ORD experiment the rotation angle ϕ changes sign, whenever the chirality or the used transmission modes change. This is always true of samples with in-plane isotropy, independent of the orientation of the molecules.

Experimental setup

The core components of the experimental setup are described elsewhere in detail.[32,33] A brief description containing the chiral-sensitive upgrade of the experimental setup is given in the following. The experimental setup is shown in Fig. 2. It consists of four different parts: a picosecond laser system, a UHV-analysis chamber, a HV-transfer and evaporation chamber, and a detection unit.

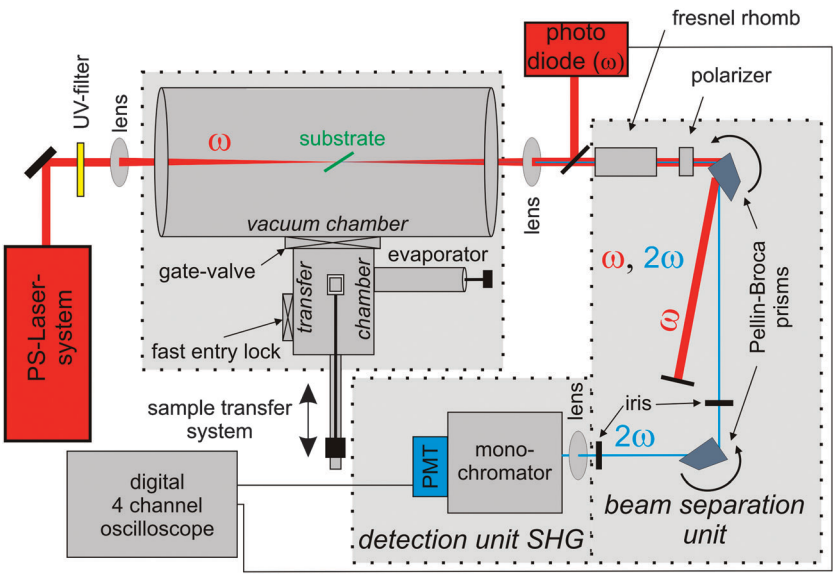

Fig. 2 Schematic view of the spectroscopic setup. The beampaths for the fundamental light (red) as well as the s-SHG light (blue) are depicted.

An optical parametric generator (Ekspla PG401-SH) is pumped by the third harmonic of a picosecond Nd:YAG laser (Ekspla PL2251A, 20 Hz) and is used as a pulsed, tuneable laser source. It emits photons in the range of 210 nm to 2.3 μm with pulse duration of about 30 ps and energies between 0.2 and 1.2 mJ per pulse at a repetition rate of 20 Hz. The fundamental laser beam passes through an SHG filter (Schott GG 435) and is focused by a lens onto a 0.8 mm^2 spot on the sample, where the second harmonic frequency is generated. Commercially available BK7 glass slabs (VWR 130 μm thick) were used as substrates for the growth of chiral molecular thin films. The substrates were cleaned using spectroscopic grade acetone before insertion into the analysis chamber and subsequently sputtered by an argon ion sputter gun for further cleaning. During the sputtering process the samples were neutralized by thermal electrons of a hot filament in order to avoid charging.[34] The transfer-chamber allows for the evaporation of molecules onto the substrate as well as for changing substrates whilst maintaining UHV-conditions in the analysis chamber. A quartz-micro-balance (Inficon SL-A1E40) allows for the determination of the coverage using Sauerbrey's equation. After transfer into the UHV-chamber (pressure is *ca.* 4×10^{-10} mbar) the sample is mounted onto a moveable *x*, *y*, *z* manipulator and can be rotated by 360°. The sample holder is cooled to liquid nitrogen temperature (77 K), which allows for measurements at constant temperature. This proved to be crucial for oppressing self-assembling effects. At room temperature crystallization of binol molecular films was observed and investigated by means of SHG microscopy.[35]

Both SHG signal and the fundamental laser beam pass through a Fresnel rhomb (B. Halle 214–450 nm) and a polarizer (Glan–Taylor prism) before being spatially separated by two rotatable Pellin–Broca prisms. In order to suppress the residual fundamental light, further wavelength selection is performed using a monochromator (LOT-Oriel, Omni-λ 300). The remaining SHG photons are detected using a photomultiplier tube (Hamamatsu, H9305-03) and recorded using a 4-channel oscilloscope (LeCroy, Waverunner 6051). The Fresnel rhomb can be rotated using a stepper motor (Newport AG-PR100P) from 0 to 340 degrees. A homemade LabView program allows for fully automated ORD-SHG measurements, as well as for fully automated SHG-wavelength scans. The Pellin–Broca prisms, the monochromator and the laser are all synchronized. The ORD-SHG measurements are performed by rotating the Fresnel rhomb from 0 to 340 degrees whilst recording the intensity of the SHG signal. This rotation of the Fresnel rhomb causes the polarization of the incoming SHG signal to rotate from 0 to 680 degrees. The polarizer splits the SHG light into p- and s-polarized light, and only p-polarized light is passed. For measuring an ORD-SHG spectrum 50 to 100 pulses are recorded and averaged at each angle in order to reduce noise. The angle between p-polarized light and the emitted SHG light (rotation angle ϕ) can then be determined by analysing the resulting intensity curve.

Results

In Fig. 3 a SHG-spectrum of binol molecules evaporated onto BK7 glass is shown.[36] No shift of the investigated resonance

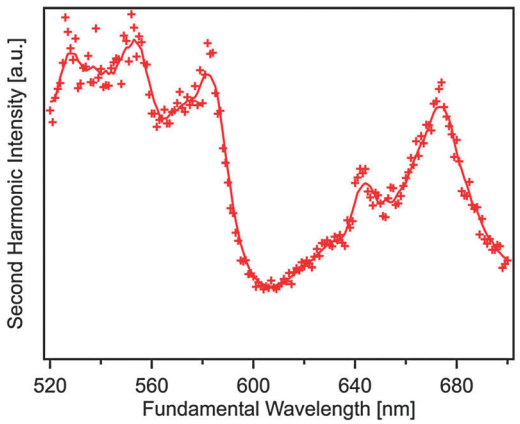

Fig. 3 SHG spectrum of evaporated binol molecules on BK7.

(337 nm) was observed for different coverages. All of the following SHG-ORD measurements were performed at a resonance wavelength of 337 nm (674 nm fundamental wavelength). As a first measurement the SHG signal from the bare BK7 substrate as a function of the incident angle is recorded at 674 nm fundamental wavelength as shown in Fig. 4. Therefore, interference of the SHG signal from the front- and backside of the substrate occurs and can be observed (for details, refer to ref. 36). Incident angles of destructive interference slightly shift for different substrates due to slight differences in thickness at different positions on the substrate. For simplicity a polarization scan of the SHG signal of the pure substrate is taken at an angle of constructive interference to define the 0° polarization angle (p-polarization) of the SHG light (there is no SHG-ORD effect of BK7). Note that racemic binol showed, as expected, the same results. Afterwards, the substrate is taken into the transfer chamber where enantiomerically pure binol is evaporated onto its cooled surface. After evaporation the substrate is transferred back into the UHV chamber and an additional incident angle dependent measurement is performed.

Two points should be mentioned here. First, since only the orthogonal part of the oscillation with respect to the substrate surface is SHG active and the parallel oscillation remains SHG

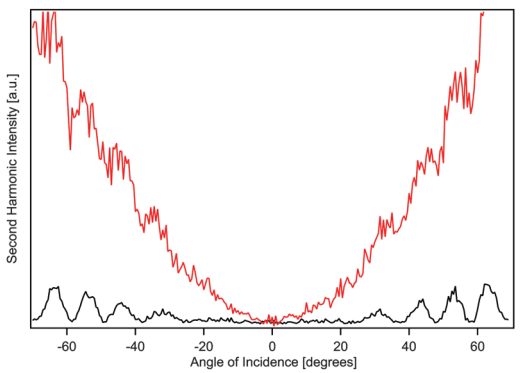

Fig. 4 Incident angle measurement for both pure BK7 substrate (black) and BK7 with deposited binol molecules (red). No signal was measured at normal incidence.

inactive there is no signal at normal incidence. The absence of SHG signal at normal incidence indicates that there are no measurable contributions from the bulk, both for the substrate and for the molecular film.[36] Second, the incident angle scan of the sample with the evaporated molecules additionally shows the interference pattern of the pure substrate. Consequently great care must be taken to measure polarization scans at angles of destructive interference of the bare substrate in order to suppress any residual SHG light from the pure substrate. We conclude that under cooled UHV conditions no electric dipole moment orthogonal to the surface is probed; thus molecules do not contribute to the SHG signal. Under ambient conditions and at room temperature, however, molecules form crystal-like structures which lead to a distinct SHG signal at 0 degree.[35]

The following incident angle dependent measurements were performed at incident angles of destructive interference. First, both enantiomers were evaporated and polarization scans were performed at different incident angles consecutively. The results for incident angles of *ca.* 35 degrees are depicted in Fig. 5. It can be seen that the phase shift (*ca.* 33 degrees) is symmetric for both enantiomers, which is a strong indication of randomly oriented molecules on the surface (with in-plane isotropy). All results are stable over time and do not appear to be influenced by the laser; neither photobleaching nor photodegradation could be observed. The measured data were fitted with a sine function and the difference in phase to p-polarized light gives the polarization angle ϕ. Best results were obtained by rotating the Fresnel rhomb over 340°, as shown in Fig. 5. Reproducing the results led to an error of rotation angle of less than 2°. The phase difference between the *R*- and *S*-enantiomers shows values of up to 75° at 674 nm.

In Fig. 6 polarization scans of evaporated *R*-binol films at different incident angles are shown. Two effects can be observed for increasing incident angles. First, the overall SHG intensity increases. This is due to the incident angle dependency of the SHG signal. Second, the phase difference between the p-polarized reference signal and the measured SHG signal

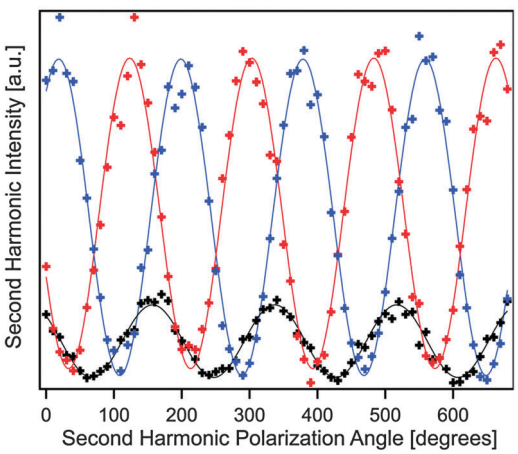

Fig. 5 *R*-Binol (red) and *S*-binol (blue) polarization scans and sine-fit. The reference signal is given by the BK7 substrate (black) and thus defines the p-polarized light (see text).

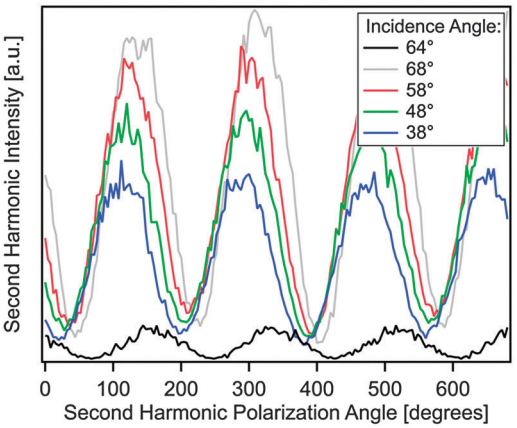

Fig. 6 Polarization scans of *R*-binol for transmission mode A for different incident angles (see text). The black graph originates from the bare BK7-substrate.

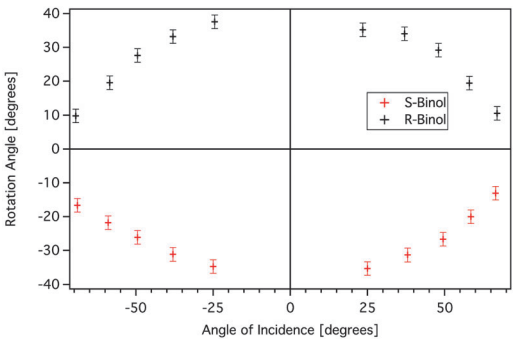

Fig. 7 Rotation angle for transmission mode A at different incident angles (see text).

of the molecules (rotation angle ϕ) decreases. The rotation angles for different incident angles and both enantiomers are presented in Fig. 7 (for transmission mode A). The high quality of the measurements is confirmed by the completely symmetric appearance of the rotation angles for the two enantiomers. Both results are in perfect agreement with theory (eqn (4)). Interchanging the enantiomers leads to a change of sign of the chiral tensor component χ_4 and hence to a change of sign of the rotation angle ϕ.

Additionally, coverage dependent SHG-ORD measurements were performed for both transmission modes mentioned earlier. The results for *S*-binol are shown in Fig. 8 and 9. The rotation angle varies significantly with the coverage. It increases up to a coverage of approximately 5×10^{16} molecules per cm^2 and then remains constant. Taking the amplitude of every fit leads to Fig. 9. The intensity increases linearly with coverage. Even at the highest coverage, no signal was observed at an incident angle of 0 degree. Thus we conclude that all molecules contribute to the SHG signal but are randomly oriented with in-plane isotropy.

Taking the rotation angle for different incident angles and different coverages, one can estimate the ratio of chiral to achiral tensor components using eqn (4). The calculated data

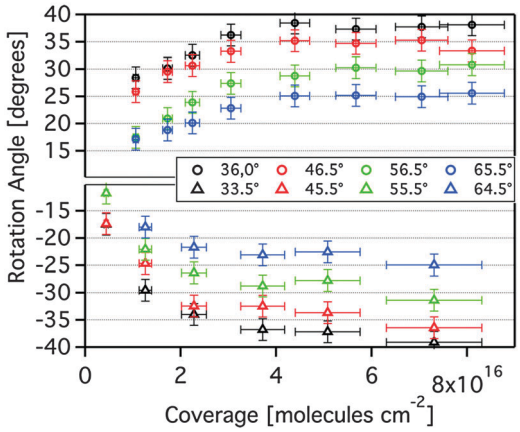

Fig. 8 Rotation angle of *S*-binol as a function of coverage for different incident angles at 674 nm. Transmission mode B (positive values) as well as transmission mode A (negative values) are shown. A clear increase of the rotation angle as well as saturation at *ca.* 5×10^{16} molecules per cm^2 can be observed.

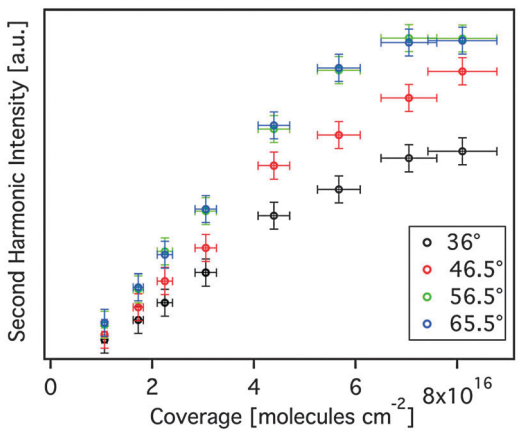

Fig. 9 Signal intensity *vs.* coverage for different incident angles.

are plotted in Fig. 11. It can clearly be seen that the ratio increases with coverage and remains constant at a certain coverage of 5×10^{16} molecules per cm^2. The reason for this behaviour can presumably be attributed to small changes in molecular orientation with increasing surface coverage. For a SHG signal three conditions must be fulfilled on a molecular level within the electric dipole approximation. First, the energy of the excitation source must be close to the electric dipole transition moment of the molecules. Second, the polarization of the excitation source must match the orientation of the electric dipole transition moment. And third, inversion symmetry must be broken for this transition dipole moment.

Note that due to the sample preparation the molecules might adsorb quite strongly (in a covalent fashion), which hinders mobility. The first layer of binol molecules is probably oriented with the hydroxyl group towards the polar surface of the amorphous BK7 substrate. In this case the electron dipole moment for the transition at 674 nm (337 nm) is mainly oriented in the *x*–*y* direction, parallel to the surface.[6] Therefore no signal

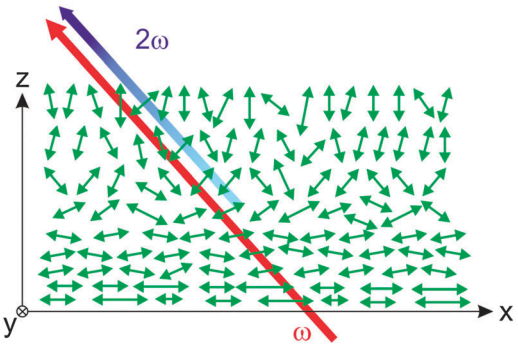

Fig. 10 2-Dimensional sketch of the proposed layer model. The dipole moments are oriented parallel to the surface for the first layers. The ordered structure vanishes with increasing coverage.

can be observed for this transition since the inversion symmetry is not broken due to the symmetric overall potential. For incident angles unequal to zero however no transition moment perpendicular to the surface can be probed. In conclusion, no signal can be observed for a small coverage up to approximately 5×10^{15} molecules per cm^2. Assuming binol molecules of the first layer to have a size (projection of the molecule profile onto the surface) of *ca.* 0.5 nm^2 this film thickness corresponds to *ca.* 10 monolayers. This is however a raw estimation and strongly depends on the orientation of the molecules.

For a higher coverage, however, the orientation of the molecules slightly changes and the transition moment at 337 nm can be probed for incident angles unequal to zero. The aforementioned ordered structure for the first layer(s) vanishes with increasing coverage (see Fig. 10). Note that there is always a higher ordered structure towards the surface and a less ordered structure in the *z*-direction for each molecule. Therefore, the molecules are embedded in an anharmonic asymmetric potential in the *z*-direction, which is a crucial condition for the generation of second harmonic light. The orientation changes by coverage, which leads to an increase of the rotation angle of the SHG-ORD signal until saturation. Because no signal is observed at incident angles of zero degree, even at highest coverage, in-plane isotropy is still present and there is no bulk contribution to the signal. Based on

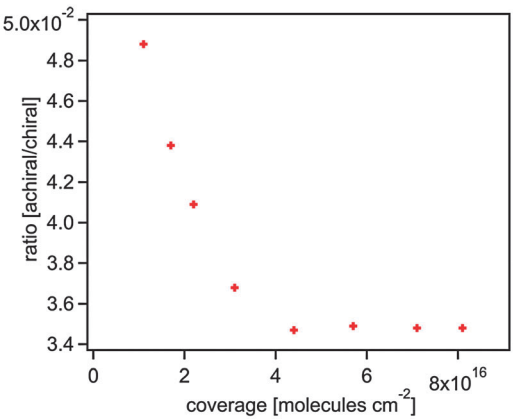

Fig. 11 Calculated ratio of achiral to chiral tensor components.

these results we conclude that the molecules reach their final orientation at a coverage above 5×10^{16} molecules per cm^2. The calculated ratio of f_s to f_p is 0.035 for this coverage.

Conclusion and outlook

In this paper the chirality of well-defined molecular films of 2,2′-dihydroxyl-1,1′binaphthyl molecules was investigated by means of the SHG-ORD effect. We used a spectroscopic setup, which allows for the investigation of supported chiral adsorbates on transparent surfaces under UHV conditions. Differences in the polarization of up to 75° were measured for different enantiomers and showed the high chiral sensitivity of this nonlinear technique. The investigated molecules are stable and do not show any self-assembling effects under these conditions. Also, no photo-bleaching or photo-degradation effects could be observed. The shown data strongly confirm the in-plane isotropy for the investigated system of these molecules, and thus support the validity of the chosen theoretical description. The rotation angle changes dramatically with coverage until saturation. We conclude that this is due to orientational effects; thus the origin of this effect lies in the different orientations of the molecules' hyperpolarizability $\alpha^{(2)}$ for different coverages. We show that coverage dependent measurements are crucial in order to understand the chiroptical response of molecular films. The data indicate that the molecules reach their final orientation at *ca.* 5×10^{15} molecules per cm^2. The ratio of chiral to achiral tensor components could be calculated and showed to change with coverage. These are important results for all further measurements of chiral molecular films under similar conditions. In recent years metal nanoparticles, protected by chiral and achiral ligands, gained much interest and showed chirality. They possess promising physical and chemical properties in the field of nanotechnology and catalysis;[29,37–39] however all these measurements were done in solutions. We hope that our results will encourage further investigations of supported chiral molecules, especially in combination with metal clusters or nanoparticles under UHV conditions. This might allow the preparation of chiral metal nanoparticles or clusters on surfaces, which would be a great step in the promising field of heterogeneous enantioselective catalysis.

Acknowledgements

This work has been supported by the European Research Council (ERC) through the advanced research grant (246645-ASC3). Financial support by the TUM Graduate School is gratefully acknowledged.

References

1 L. Kelvin, *Baltimore Lectures on Molecular Dynamics and the Wave Theory of Light*, C.J. Clay and Sons, Cambridge University Press Warehouse, 1904, p. 619.
2 S. Sioncke, T. Verbiest and A. Persoons, *Mater. Sci. Eng., R*, 2003, **42**, 115–155.
3 J. Gal, *Helv. Chim. Acta*, 2013, **96**, 1617–1657.
4 C. Logé and U. Boesl, *ChemPhysChem*, 2012, **13**, 4218–4223.
5 C. Loge and U. Boesl, *Phys. Chem. Chem. Phys.*, 2012, **14**, 11981–11989.
6 J. D. Byers and J. M. Hicks, *Chem. Phys. Lett.*, 1994, **231**, 216–224.
7 P. Fischer and F. Hache, *Chirality*, 2005, **17**, 421–437.
8 J. M. Brunel, *Chem. Rev.*, 2005, **105**, 4233.
9 J. D. Byers, H. I. Yee, T. Petralli-Mallow and J. M. Hicks, *Phys. Rev. B: Condens. Matter Mater. Phys.*, 1994, **49**, 14643–14647.
10 J. D. Byers, H. I. Yee and J. M. Hicks, *J. Chem. Phys.*, 1994, **101**, 6233–6241.
11 L. Persechini and J. F. McGilp, *Phys. Status Solidi B*, 2012, **249**, 1155–1159.
12 M. Kriech and J. Conboy, *J. Am. Chem. Soc.*, 2005, **127**, 2834–2835.
13 F. Hache, H. Mesnil and M. C. Schanne-Klein, *J. Chem. Phys.*, 2001, **115**, 6707–6715.
14 M. Kauranen, T. Verbiest, J. J. Maki and A. Persoons, *J. Chem. Phys.*, 1994, **101**, 8193–8199.
15 S. V. Elshocht, T. Verbiest, M. Kauranen, A. Persoons, B. M. W. Langeveld-Voss and E. W. Meijer, *J. Chem. Phys.*, 1997, **107**, 8201–8203.
16 M. Kauranen, T. Verbiest and A. Persoons, *J. Nonlinear Opt. Phys. Mater.*, 1999, **08**, 171–189.
17 Y. R. Shen, *Annu. Rev. Phys. Chem.*, 1989, **40**, 327–350.
18 N. Mukherjee, R. A. Myers and S. R. J. Brueck, *J. Opt. Soc. Am. B*, 1994, **11**, 665–668.
19 V. Mizrahi and J. E. Sipe, *J. Opt. Soc. Am. B*, 1988, **5**, 660–667.
20 M. Thämer, A. Kartouzian, P. Heister, T. Lünskens, S. Gerlach and U. Heiz, *Small*, 2014, DOI: 10.1002/smll.201303158.
21 T. Petralli-Mallow, T. M. Wong, J. D. Byers, H. I. Yee and J. M. Hicks, *J. Phys. Chem.*, 1993, **97**, 1383–1388.
22 M. M. Kauranen, T. Verbiest, A. Persoons, E. W. Meijer, M. N. Teerenstra, A. J. Schouten, R. J. M. Nolte and E. E. Havinga, *Adv. Mater.*, 1995, **7**, 641–644.
23 M. Kauranen, T. Verbiest, S. van Elshocht and A. Persoons, *Opt. Mater.*, 1998, **9**, 286–294.
24 T. Verbiest, M. Kauranen, A. Persoons, M. Ikonen, J. Kurkela and H. Lemmetyinen, *J. Am. Chem. Soc.*, 1994, **116**, 9203–9205.
25 V. K. Valev, *Langmuir*, 2012, **28**, 15454–15471.
26 A.-M. Pena, T. Boulesteix, T. Dartigalongue and M.-C. Schanne-Klein, *J. Am. Chem. Soc.*, 2005, **127**, 10314–10322.
27 T. G. Schaaff and R. L. Whetten, *J. Phys. Chem. B*, 2000, **104**, 2630–2641.
28 M. Farrag, M. Tschurl, A. Dass and U. Heiz, *Phys. Chem. Chem. Phys.*, 2013, **15**, 12539–12542.
29 M. Farrag, M. Tschurl and U. Heiz, *Chem. Mater.*, 2013, **25**, 862–870.

30 T. F. Heinz, H. W. K. Tom and Y. R. Shen, *Phys. Rev. A*, 1983, **28**, 1883–1885.
31 Y. R. Shen, *The principles of nonlinear optics*, 2003.
32 M. Thämer, A. Kartouzian, P. Heister, S. Gerlach, M. Tschurl, U. Boesl and U. Heiz, *J. Phys. Chem. C*, 2012, **116**, 8642–8648.
33 A. Kartouzian, M. Thamer, T. Soini, J. Peter, P. Pitschi, S. Gilb and U. Heiz, *J. Appl. Phys.*, 2008, **104**, 124313.
34 A. Kartouzian, M. Thämer and U. Heiz, *Phys. Status Solidi B*, 2010, **247**, 1147–1151.
35 M. Vanbel, S. Vandendriessche, M. A. van der Veen, D. Slavov, P. Heister, R. Paesen, V. K. Valev, M. Ameloot and T. Verbiest, *Proc. SPIE*, 2013, **8770**, 87701F.
36 A. Kartouzian, P. Heister, M. Thämer, S. Gerlach and U. Heiz, *J. Opt. Soc. Am. B*, 2013, **30**, 541–548.
37 C. Gautier and T. Bürgi, *ChemPhysChem*, 2009, **10**, 483–492.
38 I. Dolamic, S. Knoppe, A. Dass and T. Bürgi, *Nat. Commun.*, 2012, **3**, 798.
39 C. Noguez and I. L. Garzon, *Chem. Soc. Rev.*, 2009, **38**, 757–771.

